

VP23R of Infectious Spleen and Kidney Necrosis Virus Mediates Formation of Virus-Mock Basement Membrane To Provide Attaching Sites for Lymphatic Endothelial Cells[∇]

Xiaopeng Xu,¹ Shaoping Weng,¹ Ting Lin,¹ Junliang Tang,¹ Lichao Huang,¹ Jing Wang,¹
Xiaoqiang Yu,² Ling Lu,¹ Zhijian Huang,¹ and Jianguo He^{1,*}

State Key Laboratory of Biocontrol, School of Life Sciences, Sun Yat-sen (Zhongshan) University, Guangzhou, China,¹ and
Division of Cell Biology and Biophysics, School of Biological Science, University of Missouri-Kansas City, Kansas City, Missouri²

Received 6 May 2010/Accepted 19 August 2010

Putative open reading frames (ORFs) encoding laminin-like proteins are found in all members of the genus *Megalocytivirus*, family *Iridoviridae*. This is the first study that identified the VP23R protein encoded by ORF23R of the infectious spleen and kidney necrosis virus (ISKNV), a member of these genes of megalocytiviruses. The VP23R mRNA covering the ISKNV genomic coordinates 19547 to 22273 was transcribed ahead of the major capsid protein. Immunofluorescence analysis demonstrated that VP23R was expressed on the plasma membrane of the ISKNV-infected cells and could not be a viral envelope protein. Residues 292 to 576 of VP23R are homologous to the laminin γ 1III2-6 fragment, which covers the nidogen-binding site. An immunoprecipitation assay showed that VP23R could interact with nidogen-1, and immunohistochemistry showed that nidogen-1 was localized on the outer membrane of the infected cells. Electron microscopy showed that a virus-mock basement membrane (VMBM) was formed on the surface of the infected cells and a layer of endothelial cells (ECs) was attached to the VMBM. The VMBM contained VP23R and nidogen-1 but not collagen IV. The attached ECs were identified as lymphatic endothelial cells (LECs), which have unique feature of overlapping intercellular junctions and can be stained by immunohistochemistry using an antibody against a specific lymphatic marker, Prox-1. Such infection signs have never been described in viruses. Elucidating the functions of LECs attached to the surface of the infected cells may be useful for studies on the pathogenic mechanisms of megalocytiviruses and may also be important for studies on lymphangiogenesis and basement membrane functions.

Basement membrane (BM), a dense and sheetlike structure that is always associated with cells, is a very important specialized form of extracellular matrix (31, 67). BMs mediate tissue compartmentalization and provide structural support to the epithelium, endothelium, peripheral nerve axons, fat cells, and muscle cells, as well as structural and functional foundations of the vasculature (25, 31, 52). BM is also an important regulator of cell behaviors, such as adhesion, migration, proliferation, and differentiation. BMs are highly cross-linked and insoluble materials. They are highly complex and are made up of more than 50 known components (31, 54). Although the molecular composition of BMs is unique in each tissue, their basic structures are similar. Even if many more isoforms exist in different species, the major BM proteins and their receptors are conserved from *Caenorhabditis elegans* to mammals. BM consists of a layer of laminin polymer, a layer of type IV collagen network, and the nidogen protein, which acts as a cross-linker of these two networks. Other BM components, such as perlecan and fibulin, interact with the laminin polymer and the type IV collagen network to organize a functional BM on the basolateral aspect of the cells (31, 45, 52).

The components of BM are able to self-assemble and form

a sheetlike structure, and laminin is the key molecule in this process (50). Laminin protein consists of three different chains (α , β , and γ), which comprise a cross-shaped molecular structure with three short amino-terminal arms and a long carboxyl-terminal triple-helical arm (58, 68). The three short arms of this cross-shaped structure can interact with each other in the presence of calcium. Through the binding of globular G domain at the carboxyl-terminal end of the α chain to the cell receptors (e.g., integrins and dystroglycans), laminin self-assembles into polygonal lattices on cell surfaces. This process initiates BM self-assembly (15, 21, 25, 38, 65, 66). To date, 17 laminin isoforms have been observed in different tissues (51). Among them, laminin-1, the crux of early embryonic BM assembly, has been well studied. Laminin-1 consists of α 1, β 1, and γ 1 chains and can interact with nidogen-1 with high affinity through a laminin-type epidermal growth factor-like (LE) module, γ 1III4, within the domain III of the γ 1 chain (1, 42). The heptapeptide “NIDPNAV” within the γ 1III4 motif of laminin-1 is essential for the interaction between laminin-1 and nidogen-1 (41, 46). Blocking the interactions between laminin-1 and nidogen-1 leads to the disruption of BMs. This indicates that the formation of laminin/nidogen complex is essential for BM assembly and stability (30, 61). Nidogen-1, also called entactin-1, is a dumbbell-shaped sulfated 150-kDa glycoprotein consisted of three domains (G1, G2, and G3) (12). By interacting with collagen IV through its G2 domain and binding with laminin γ 1 chain through its G3 domain, nido-

* Corresponding author. Mailing address: School of Life Sciences, Sun Yat-sen (Zhongshan) University, Guangzhou 510275, People's Republic of China. Phone: 86 20 84113793. Fax: 86 20 84113229. E-mail: lsshjg@mail.sysu.edu.cn.

[∇] Published ahead of print on 1 September 2010.

gen-1 bridges the layers of the laminin network and the collagen IV network to construct the fundamental structure of BMs (48). Collagen IV is a triple-helical trimer composed of three α chains. Through the hexamer formation of the carboxyl-terminal globular non-collagenous-1 (NC1) domain of each α chain, two collagen IV proteins assemble into a dimer. Dimers of collagen IV connect with each other via their amino-terminal 7S domains and self-assemble into a network (24, 27, 31, 32). Six kinds of α chains of collagen IV have been identified in mammals. Among them, $\alpha 1$ and $\alpha 2$ chains are the most abundant forms of collagen IV found in all BMs (19, 23). They commonly form a collagen IV molecule with a $\alpha 1$ and $\alpha 2$ ratio of 2:1 (31, 35).

Iridoviruses infect invertebrates and poikilothermic vertebrates, including insects, fish, amphibians, and reptiles. These viruses are a group of icosahedral cytoplasmic DNA viruses with circularly permuted and terminally redundant DNA genomes (6, 8, 9, 10, 57, 62). The family *Iridoviridae* has been subdivided into five genera: *Iridovirus*, *Chloriridovirus*, *Ranavirus*, *Lymphocystivirus*, and *Megalocystivirus* (7). The genus *Megalocystivirus*, characterized by the ability to cause swelling of the infected cells, is one group of the most harmful viruses to cultured fish (7, 26, 29). Infectious spleen and kidney necrosis virus (ISKNV), the causative agent of a disease that causes high mortality rates in farmed mandarin fish, *Siniperca chuatsi*, and large-mouth bass, *Micropterus salmoides*, is regarded as the type species of *Megalocystivirus* (7). Similar to infection caused by other members of the *Megalocystivirus*, fish ISKNV infection is characterized by cell hypertrophy in the spleen, kidney, cranial connective tissue, and endocardium (16, 17). Aside from mandarin fish and large-mouth bass, ISKNV-like virus can also be detected in the tissues of more than 60 marine and freshwater fishes (14, 28, 59, 64). The entire genome of ISKNV has been sequenced, and the organization of open reading frames (ORFs) of ISKNV was analyzed by using DNASTAR Omega 2.0 and Genescan (18). The ISKNV genome is about 110 kbp and contains 125 putative ORFs (GenBank accession no. AF371960).

Putative ORFs, encoding viral proteins containing a fragment homologous to laminin and a putative transmembrane fragment, were found in all of the sequenced genomes of the members of *Megalocystivirus*. These ORFs include ORF23R of ISKNV (GenBank accession no. AAL98747), laminin-like protein gene of olive flounder iridovirus (GenBank accession no. AAT76907), ORF2 of sea perch iridovirus (GenBank accession no. AAV51313), predicted laminin-type epidermal growth factor-like protein of large yellow croaker iridovirus (GenBank accession no. ABI32391), an unknown gene of red sea bream iridovirus (GenBank accession no. AAQ07956), ORF2 of rock bream iridovirus (GenBank accession no. AAN86692), and laminin-type epidermal growth factor-like protein of orange-spotted grouper iridovirus (GenBank accession no. AAX82335). These putative proteins are highly homologous to each other in amino acid sequence (65 to 99% identity). However, the functions of these proteins have never been identified. This is the first study to identify that the VP23R protein encoded by ORF23R of ISKNV is a plasma membrane-localized viral protein. In addition, we discovered a new function of VP23R in a unique pathological phenomenon of virus infection: the attachment of lymphatic endothelial cells (LECs) to

the infected cells. Nidogen-1 assisted VP23R in the construction of a BM-like structure, providing an attachment site for LECs. This unique pathological phenomenon has never been found in viruses and is an attractive direction for studies of pathogenic mechanisms of megalocystiviruses. Moreover, studies on the unique profiles of the virus-mock BM can help us learn more about the functions of BM components and the mechanisms of lymphangiogenesis.

MATERIALS AND METHODS

Fish and virus. Mandarin fish were from a local fish farm in Guangzhou City, Guangdong Province, China, and were kept in separate tanks at 28°C. Tank water was filtrated through a sand and carbon layer and aerated before use. ISKNV was purified from diseased mandarin fish identified in our laboratory (16) and propagated in cultured mandarin fish fry cell line (MFF-1) (11). The supernatants of the cultured cells at 6 days postinfection (dpi) of ISKNV were collected, and the virus titer was determined by using the 50% tissue culture infective dose (TCID₅₀) method as described previously (11).

5'- and 3'-RACE. Total RNA was isolated from spleens of ISKNV-infected mandarin fish. The 5' and 3' ends of ORF23R transcript were mapped by using a GeneRacer kit (Invitrogen) according to the manufacturer's instructions. 5'-Rapid amplification of cDNA ends (RACE)-PCR amplification was performed with GeneRacer 5'-RACE primer and ORF23R specific reverse primer (5'-GC AGTTGCCGCTCAAACACTCTGG-3'). Nested PCR was subsequently performed with GeneRacer 5'-RACE nested primer and ORF23R nested primer (5'-CACTCCATGTTTCAGGACTTCGCTGC-3') by using the first-round PCR product as a template. 3'-RACE-PCR was performed by using GeneRacer 3'-RACE primer, together with an ORF23R-specific forward primer (5'-GTCAT TGGGTCTGCATGGTTGCCGC-3'). The PCR products were subcloned into the PMD19-T TA vector (TaKaRa, China) and sequenced.

cDNA of mandarin fish BM components. A series of partial cDNA of mandarin fish BM components were cloned, sequenced, and submitted to GenBank. Briefly, RNA was extracted from kidneys of healthy mandarin fish by using the TRIzol method, and the first-strand cDNA was synthesized by using SuperScript III RT (Invitrogen). A specific forward primer (5'-CAGCTGTAAGCCAGGA GTGA-3') and reverse primer (5'-ACCTGTGCTCTGACCAGGCTGTA-3') were designed based on the known laminin $\gamma 1$ -chain coding sequences of green-spotted pufferfish (*Tetraodon nigroviridis*) and zebrafish (*Danio rerio*) and used to amplify the laminin $\gamma 1$ fragment of mandarin fish (GenBank accession no. HM153806) by reverse transcription-PCR (RT-PCR). The primers MNi1 (5'-T ACCAGTGGCGTCAGACCATCACCTTCC-3') and MNi2 (5'-CGGTCCGTTG GGACATCTGCAGG-3') were designed based on the known human, zebrafish, and green-spotted pufferfish nidogen-1 G2/G3 domains coding sequences for amplification of mandarin fish nidogen-1 (GenBank accession no. HM138201). A collagen IV $\alpha 1$ fragment from mandarin fish (GenBank accession no. HM138202), which is orthologous to residues 1408 to 1607 of human collagen IV $\alpha 1$ (GenBank accession no. CAM14222) was amplified by using A1-1 (5'-CCG GGCCCTCCTCAATG-3') and A1-2 (5'-GGTAGCAAAGCCAGAAGCTGTG-3') primers. A collagen IV $\alpha 2$ fragment from mandarin fish (GenBank accession no. HM138203), which is orthologous to residues 1488 to 1667 of human collagen IV $\alpha 2$ (NCBI accession no. NP_001837) was amplified by using A2-1 (5'-ATGCC GGGCCGCGTCAGC-3') and A2-2 (5'-CAGAGCTGAGCCAGAAGCT GTGCTTGT-3') primers. All cDNA fragments were cloned into PMD-19T vector and sequenced.

Antibody preparation. A DNA fragment corresponding to amino acid residues 18 to 169 of VP23R was amplified and cloned into the PQE30 vector (Qiagen) (referred to as PQE30-XF23 vector). The recombinant vector was transformed into the M15 *Escherichia coli* strain (Qiagen) to express 6×His-XF23 fusion protein. The protein was purified with Ni-NTA and separated by electrophoresis in 15% sodium dodecyl sulfate (SDS)-polyacrylamide gels. The gel slice containing 6×His-XF23 band was cut out and ground with adjuvant to immunize BALB/c mice. Full-length ISKNV major capsid protein (MCP) gene (ORF006L) was cloned into the PRSET-A vector (Invitrogen). Recombinant MCP was expressed in *E. coli* strain BL21(DE3) (Novagen), purified, and used as an antigen to immunize rabbits. Mandarin fish nidogen-1 G3 domain was expressed in PMAL-C2X vector (NEB, United Kingdom) in *E. coli Origami* strain (Novagen). The MBP tag was cut out by Factor Xa (NEB, United Kingdom), and nidogen-1 G3 fragment was separated by SDS-PAGE. Then, nidogen-1 G3 bands were cut out to immunize BALB/c mice. The collagen IV $\alpha 1$ and $\alpha 2$ fragments were cloned into the PRSET-A vector and expressed in BL21(DE3), and recom-

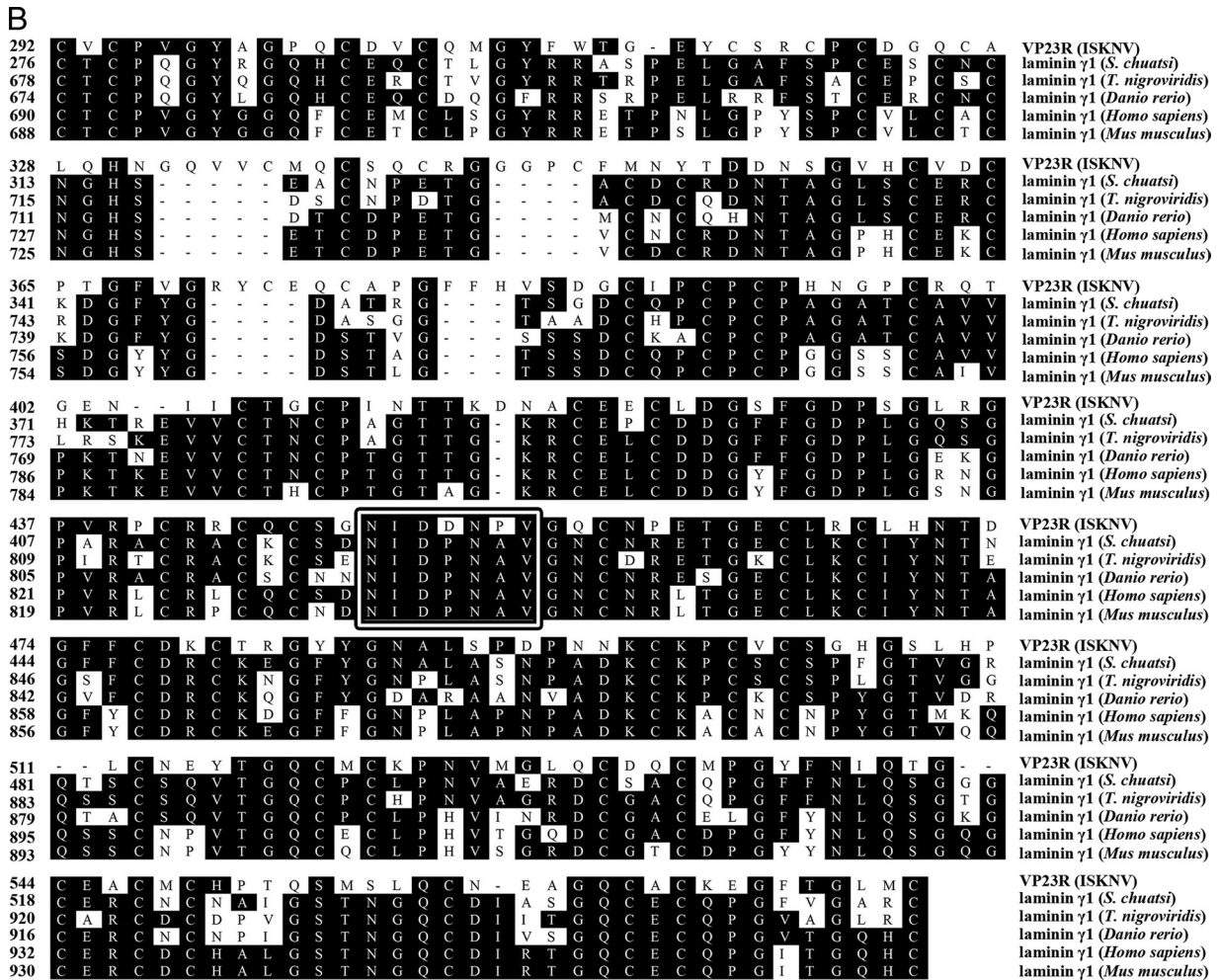


FIG. 1—Continued.

quences of VP23R, VPΔ23, and VP23LN were cloned into PEGFP-N3 (Clontech) and pCDNA 3.1/V5-His A (Invitrogen), generating PN-23/PN-Δ23/PN-23LN and PC-23/PC-Δ23/PC-23LN, which express green fluorescent protein (GFP)- and V5-tagged proteins, respectively. The full-length *T. nigroviridis* nidogen-1 (GenBank accession no. HM138204) was cloned into PEGFP-N3 and pCDNA 3.1/V5-His A, generating PN-Ni and PC-Ni that express GFP- and V5-tagged nidogen-1, respectively. For coimmunoprecipitation, PC-Ni was cotransfected with PN-23, PN-Δ23, or PN-23LN into fathead minnow (FHM) fish cells. For reciprocal coimmunoprecipitation, PC-23, PC-Δ23, or PC-23LN was cotransfected with PN-Ni into FHM cells. After 72 h, cells were collected and lysed. Coimmunoprecipitation and reciprocal coimmunoprecipitation were performed by using anti-V5 agarose affinity gel (Sigma). Western blotting was performed with rabbit anti-GFP antibody (Sigma) and alkaline phosphatase-conjugated goat anti-rabbit secondary antibodies (Sigma).

Coimmunoprecipitation assays were also performed with the ISKNV-infected spleens of mandarin fish. Briefly, spleens from the ISKNV-infected mandarin fish at 5 dpi were homogenized and lysed. Coimmunoprecipitation was performed using 5 μl of anti-VP23R mouse polyclonal antibodies and 50 μl of a suspension of protein A/G-Sepharose (Santa Cruz). Western blotting was performed with anti-nidogen-1 rabbit polyclonal antibodies.

Electron microscopy analysis. Spleens of the ISKNV-infected mandarin fish were fixed in 2.5% glutaraldehyde in 0.1 M phosphate buffer (pH 7.4). Specimens were then rinsed with 0.1 M phosphate buffer four times, postfixed in 0.1 M phosphate buffer containing 2.0% osmium tetroxide for 1 h at 4°C, and embedded in Epon's 812 after dehydration. Ultrathin sections were cut and stained with uranyl acetate and lead citrate. They were then examined on a Philips CM10 electron microscope.

RESULTS

Structural and bioinformatics analyses of ORF23R. 5'-RACE showed that the transcription starting site of ORF23R was at the ISKNV genomic coordinate 19547, which extended only 14-bp upstream of ORF23R. 3'-RACE showed that the ORF23R mRNA contained a typical poly(A) tail and the transcription ended at 22273, extended 140 bp downstream of ORF23R. A computer-assisted analysis of the ISKNV genome indicated that ORF23R began at nucleotide 19562 and terminated at nucleotide 22132, which encoded a putative protein of 856 amino acids with an apparent molecular mass of 90.7 kDa and an isoelectric point of 4.8. The protein, designated VP23R, was predicted to have a 17-residue signal peptide and a potential transmembrane domain localized between residues 818 and 840. Eight N-glycosylation and six O-glycosylation sites were predicted in the entire protein sequence. Therefore, VP23R protein may retain characteristics of a membrane protein, presenting a large N-terminal ectodomain, a C-terminal hydrophobic anchor, and a short C-terminal cytoplasmic tail with only 16 residues (Fig. 1A).

An initial BLAST search showed that residues 292 to 576 of

VP23R is homologous to the γ 1III2-6 LE motifs of laminin γ 1 chain. We have cloned the mandarin fish laminin γ 1 chain fragment, including the γ 1III2-6 motifs. Sequence comparison shows that there is 44.6% identity in amino acid sequence between mandarin fish laminin γ 1III2-6 fragment and VP23R residues 292 to 576. This region (residues 292 to 576) of VP23R also shows 43.5, 41.3, 43.8, and 44.2% identity to the laminin γ 1III2-6 fragments of *T. nigroviridis* (GenBank accession no. CAD27803), *Danio rerio* (GenBank accession no. CAK05288), *Homo sapiens* (GenBank accession no. AAA59492), and *Mus musculus* (GenBank accession no. AAA39405), respectively (Fig. 1B). The γ 1III4 motif of laminin γ 1 chain is the binding site of nidogen-1. The heptapeptide NIDPNAV within γ 1III4 is essential for the interactions between laminin and nidogen-1 (41, 46). In VP23R, a homologous heptapeptide NIDDNPV was also found, and only two residues were different.

VP23R is localized on plasma membrane. In ISKNV-infected cultured MFF-1 cells, VP23R mRNA began to transcribe at 8 h postinfection, prior to transcription of MCP, which began at 36 h postinfection (data not shown). To identify the cellular location of VP23R protein, a series of mandarin fish spleen sections were prepared at 1, 2, 3, 4, 5, and 6 dpi (Fig. 2). Mice anti-VP23R polyclonal antibody, together with rabbit anti-MCP polyclonal antibody, was used to perform immunofluorescence assays on these sections. Since ISKNV is a typical cytoplasmic DNA virus and MCP of ISKNV is expressed in the cytoplasm (7), MCP staining can provide a cytoplasmic counterstaining for VP23R localization. The MCP signals (red fluorescence) were surrounded by the green fluorescence of VP23R signals (Fig. 2C and D), suggesting that VP23R is localized on the plasma membrane of the infected cells. VP23R began to appear on the membrane of the infected cells at 1 dpi (Fig. 2A), and MCP began to express inside the infected cells at 3 dpi (Fig. 2C). At 5 dpi, MCP began to release out of the infected cells (Fig. 2E, white arrow). At 6 dpi, almost all MCP was found outside of the infected cells (Fig. 2F, white arrows). On the contrary, VP23R protein appeared on the membrane during the whole infection process.

Interaction between VP23R and nidogen-1. Immunoprecipitation assays showed that VP23R and its laminin-replaced mutant exhibited affinity to nidogen-1 and could be coprecipitated by the V5-tagged nidogen-1, whereas the “NIDDNPV” deletion mutant of VP23R was not coprecipitated with nidogen-1 (Fig. 3A). Reciprocal coimmunoprecipitation showed that GFP-tagged nidogen-1 was also coprecipitated with V5-tagged VP23R and its laminin-replaced mutant but not with its “NIDDNPV” deletion mutant (Fig. 3B). To further confirm the interaction between VP23R and nidogen-1, immunoprecipitation was also performed in the spleen of the virus-infected cells (Fig. 3C). The result showed that nidogen-1 in the spleens of ISKNV-infected mandarin fish was coprecipitated with anti-VP23R polyclonal antibody, indicating that VP23R can interact with nidogen-1 *in vivo*.

Immunohistochemistry of the virus-infected spleens showed that nidogen-1 was present on the outer membranes of the ISKNV-infected cells (Fig. 4A), which were characterized by marked hypertrophy (16, 17). VP23R was expressed on the plasma membrane of the infected cells. This result confirmed that nidogen-1 interacts with VP23R in the ISKNV-infected

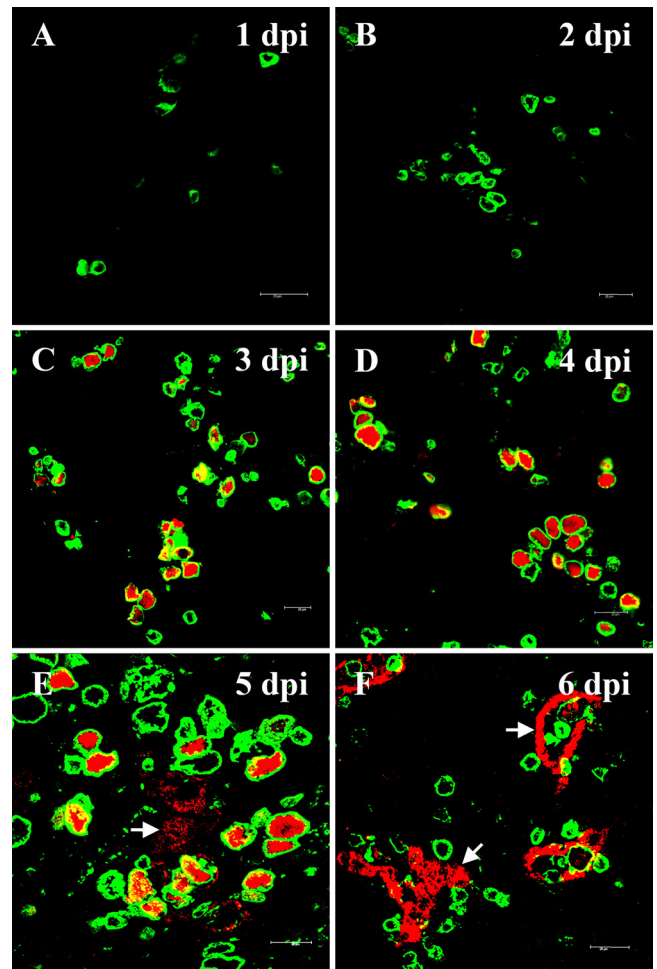


FIG. 2. Immunofluorescence analysis of spleens from ISKNV-infected mandarin fish. The infected cells are labeled with Alexa Fluor 488 for VP23R (green fluorescence), and the ISKNV particles are labeled with Alexa Fluor 633 for MCP (red fluorescence, white arrows). The spleen images are from different times postinfection as indicated. (A) 1 dpi; (B) 2 dpi; (C) 3 dpi; (D) 4 dpi; (E) 5 dpi; (F) 6 dpi. White arrows indicate the released virions.

tissues. Nidogen-1 proteins on the surface of infected cells may be recruited by VP23R. Nidogen-1 is also a ligand for collagen IV. However, no collagen IV was detected on the membrane of ISKNV-infected cells by anti-collagen IV α 1 and α 2 chain antibodies (Fig. 4C and E).

Interaction of lymphatic endothelial cells with virus-infected cells. Under the electron microscope, almost all of the ISKNV-infected cells were found to be attached with layers of flat cells (Fig. 5). The flat cells were identified by electron microscopy as endothelial cells (ECs). A low-electron-dense structure 40 to 50 nm thick existed between the plasma membranes of the infected cells and the surrounding of ECs (Fig. 5F, black arrowheads), which are always attached to the BMs. This result showed that VP23R and nidogen-1 may provide an attaching site for ECs. The 40- to 50-nm-thick structures outside of the infected cells did not show an electron-dense zone, which is present in true BMs and consists of collagen IV network (20). This confirmed that collagen IV is not present

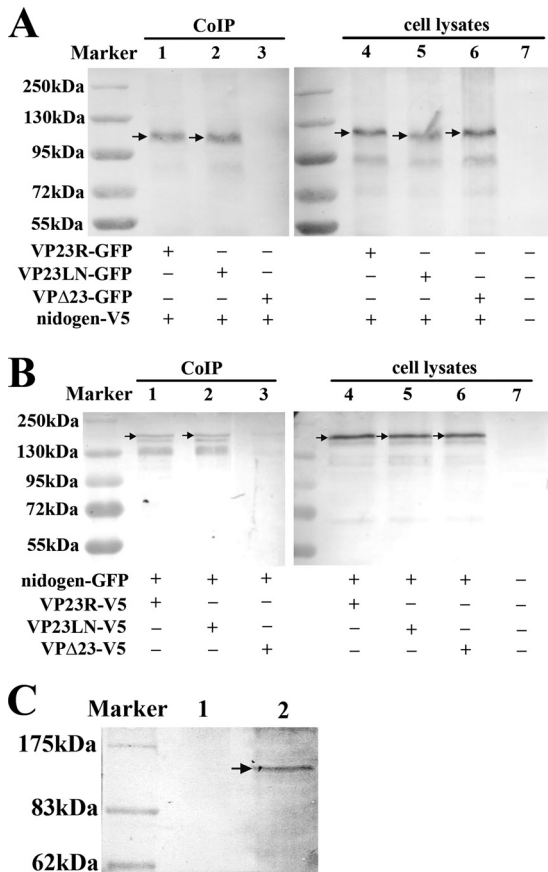


FIG. 3. (A) Coimmunoprecipitation assays in FHM cells. GFP-tagged VP23R (VP23R-GFP) (lane 1) and its laminin-replaced mutant (VP23LN-GFP) (lane 2) could be coprecipitated by the V5-tagged nidogen-1 (nidogen-V5), whereas the GFP-tagged “NIDDNPV” deletion mutant of VP23R (VPΔ23-GFP) could not be coprecipitated (lane 3). The GFP-fusion proteins in the lysates of FHM cells transfected with PC-Ni along with PN-Δ23 (lane 4), PN-23 (lane 5), or PN-23LN (lane 6) were detected by using anti-GFP antibody, whereas the lysates of the untransfected FHM cells showed no positive signals (lane 7). (B) Reciprocal coimmunoprecipitation showed that GFP-tagged nidogen-1 (nidogen-GFP) was coprecipitated by the V5-tagged VP23R (VP23R-V5) (lane 1) and its laminin-replaced mutant (VP23LN-V5) (lane 2), but was not coprecipitated by the V5-tagged “NIDDNPV” deletion mutant of VP23R (VPΔ23-V5) (lane 3). The nidogen-GFP fusion protein in the lysates of FHM cells transfected with PN-Ni, along with PC-23 (lane 4), PC-23LN (lane 5), or PC-Δ23 (lane 6), could be detected by using anti-GFP antibody, whereas the lysates of the untransfected FHM cells showed no positive signals (lane 7). (C) Immunoprecipitation assays performed in the ISKNV-infected mandarin fish spleens. Nidogen-1 (~150 kDa) was coprecipitated by anti-VP23R antibodies (lane 2, black arrow) but not by control sera (lane 1).

outside the membrane of the infected cells. These 40- to 50-nm-thick structures, composed of VP23R and nidogen-1, did not contain collagen IV α1 and α2 chains, worked in the same manner as true BMs to provide attaching sites for ECs and were termed virus-mock basement membranes (VMBM). Figure 5G and H show an infected cell releasing endocytes and mature virions.

The attached ECs showed overlapping intercellular junctions (Fig. 5A to C, black arrows), which were regarded as the

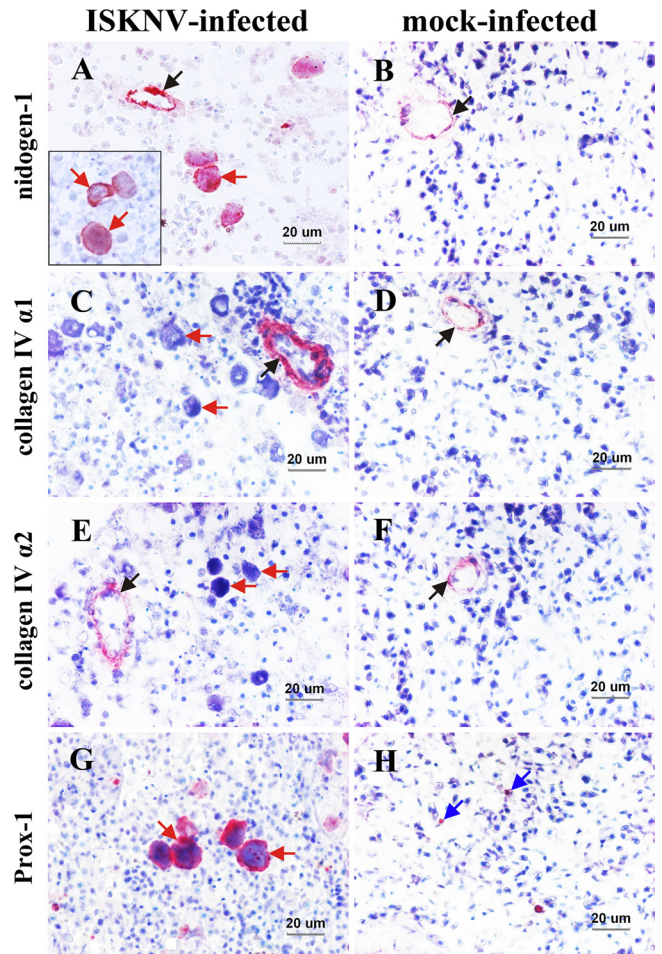


FIG. 4. Immunohistochemical assays of ISKNV- and mock-infected (as controls) mandarin fish spleens (magnification, ×400). In ISKNV-infected spleens (A, C, E, and G), the infected cells showed signs of hypertrophy (red arrows). No enlarged infected cells were observed in mock-infected spleens (B, D, F, and H). Nidogen-1 was detected on the plasma membranes of the enlarged ISKNV-infected cells (panel A and Inset, red arrows) and on true BMs (A and B, black arrows). The α1 and α2 chains of collagen IV were detected in true BMs (C, D, E, and F, black arrows), but not on the plasma membrane of the enlarged ISKNV-infected cells (C and E, red arrows). (G) Attached LECs on the plasma membranes of the enlarged ISKNV-infected cells showed prox-1 positive (red arrows). (H) LECs in mock-infected tissues showed prox-1 positive (blue arrows).

unique profile of LECs (39, 43, 63). Thus, the attached ECs can be identified as LECs. The result was confirmed by immunohistochemical assay using antibody against Prox-1 protein, a specific marker for LECs (13, 44). As a LEC-specific transcription factor, Prox-1 was specifically stained in the attached LECs (Fig. 4G).

DISCUSSION

The predicted ORF23R, located in the region from 19562 to 22132 of the ISKNV genome, encodes an 856-residue protein, termed VP23R. The putative transmembrane region near the carboxyl terminus and the putative signal peptide at the amino-terminal end make VP23R a cell plasma membrane-localized

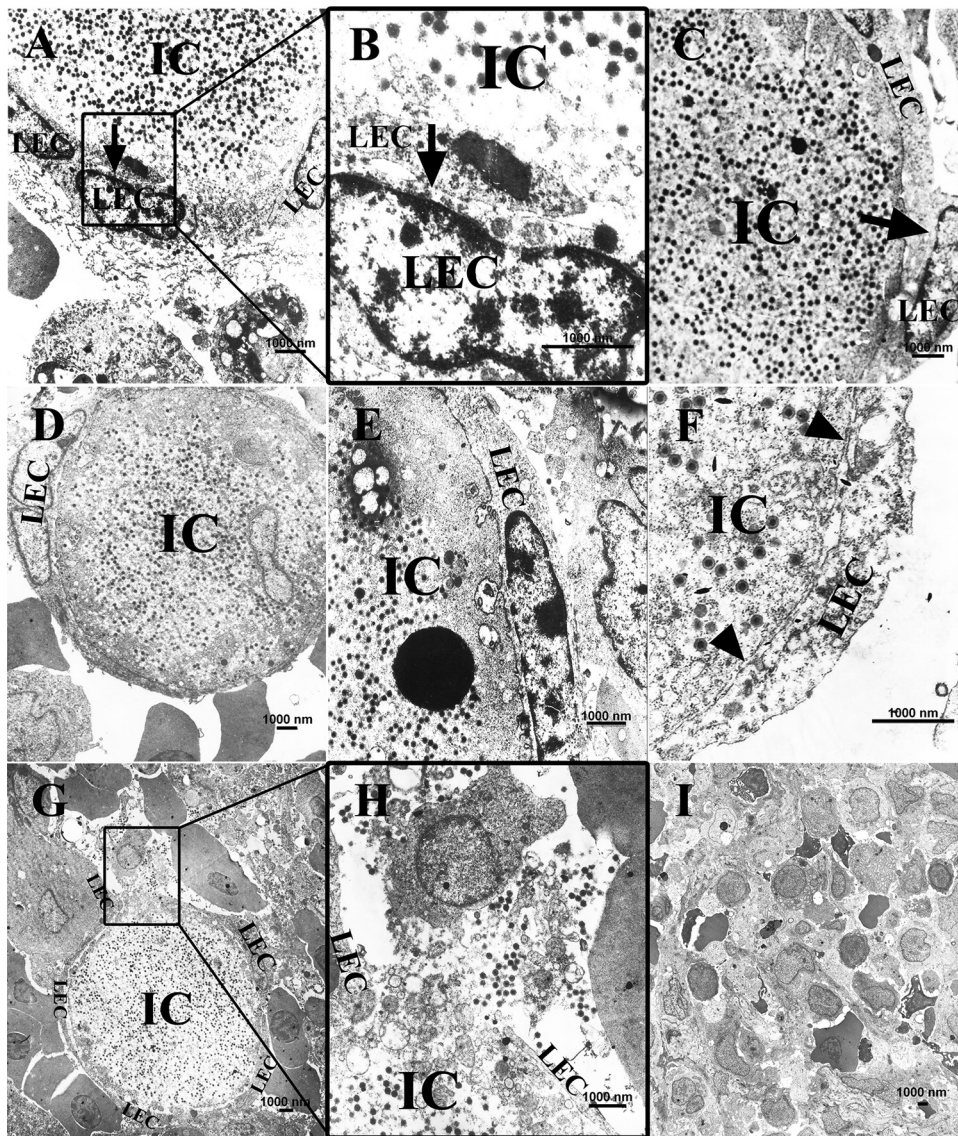


FIG. 5. Electron microscope assays of ISKNV-infected cells in the spleens of mandarin fish. ISKNV-infected cells (IC) were attached by LECs. Black arrows point to the overlapping intercellular junctions of the attached LECs; black arrowheads indicate VMBM, a low-electron-density layer. The area of the overlapping intercellular junctions of the attached LECs (magnification, $\times 6,000$) framed with black lines in panel A was enlarged in panel B. Additional magnifications are shown: $\times 6,000$ (C), $\times 4,000$ (D), $\times 8,000$ (E), and $\times 15,000$ (F). (G) In this panel (magnification, $\times 2,000$), attached LECs uncovered their surroundings, and infected cells released endocytes and mature virions. The location of the crack of the LEC “bag” is framed in black box and enlarged in panel H. (I) As controls, no infected cells were observed in the spleens of mock-infected mandarin fish (magnification, $\times 1,650$).

protein. The putative extracellular region of VP23R is homologous to the $\gamma 1$ III2-6 fragment of laminin-1 that contains the high-affinity nidogen-binding site of laminin, indicating that VP23R may have functions related to the BM. Ours is the first study to identify VP23R protein and analyze its functions in mediating formation of BM-like structures on the surfaces of ISKNV-infected cells, providing a site for LEC adhesion.

The double-stain immunofluorescence assays showed that VP23R protein was expressed earlier than MCP in the spleens of infected mandarin fish. VP23R was localized on the plasma membrane of the infected cells. The location of VP23R did not coincide with MCP, which represents virus particles. During the process of ISKNV infection, VP23R was constantly local-

ized on the plasma membrane since it was detected on the plasma membrane even after viral particles were released outside the cells. Based on these results, we infer that VP23R is a plasma membrane-localized viral protein, but it cannot be an envelope protein of ISKNV. This result also disproved the previous assumption that the accumulation of viral particles results in megalocytosis of the infected cells (7), because the infected cells enlarged without appearance of MCP.

Residues 292 to 576 of VP23R are homologous to the $\gamma 1$ chain III2-6 motifs of mandarin fish laminin with 44.6% identity, which contain the high-affinity nidogen-binding site. By using coimmunoprecipitation, we verified that VP23R could interact with nidogen-1. The heptapeptide “NIDPNAV”

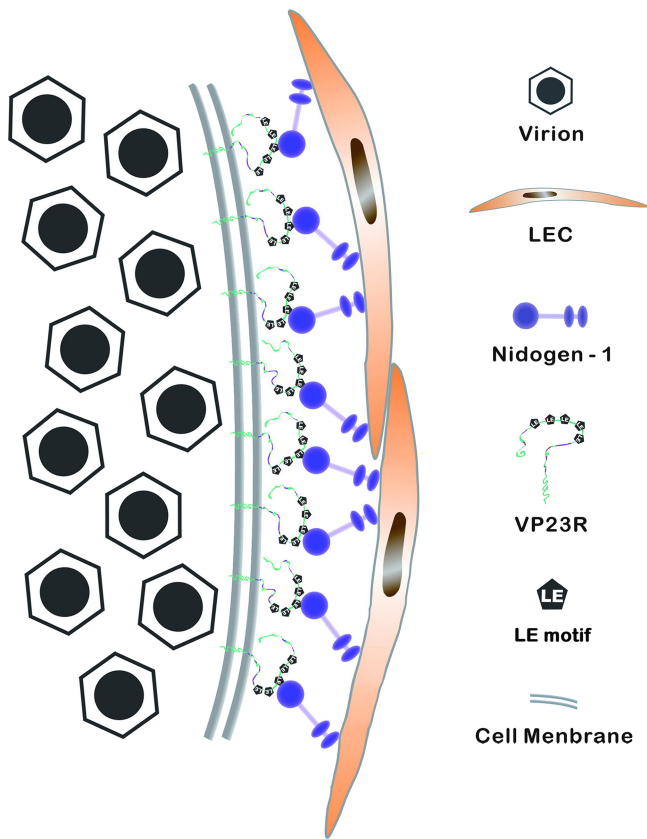


FIG. 6. Schematic illustration of VMBM. The plasma membrane of the infected cells took the roles of the laminin polymer layers of true BMs, and the laminin γ 1 chain III2-6 homologous region of VP23R mimicked the γ 1 arms that extend out of the laminin polymer layer to bind nidogen-1. VMBMs are free of collagen IV. Nidogen-1 may provide attaching sites for LECs.

within the γ 1 chain III4 motif of laminin is crucial for interaction of laminin γ 1 with nidogen-1 (41, 46). In VP23R, the heptapeptide “NIDPNAV” was substituted by “NIDDNPV,” in which only two amino acids were changed, and this alteration did not affect the interaction between VP23R and nidogen-1. Deletion of the heptapeptide “NIDDNPV” resulted in a loss of VP23R binding ability to nidogen-1. This result indicates that the heptapeptide is essential for the interaction between VP23R and nidogen-1.

Immunohistochemistry assay showed that nidogen-1 was present on cell membrane of ISKNV-infected cells. Electron microscopy showed that VP23R, along with nidogen-1, formed a low electron-density BM-like structure (VMBM), to which a layer of LECs were attached. Figure 6 shows the schematic illustration of VMBM. In VMBM, the plasma membrane of the infected cells take the roles of the laminin polymer layer of true BMs, which always binds to cell receptors and initiates BM self-assembly. The laminin γ 1 chain III2-6 homologous region of VP23R mimics the γ 1 short arms that extend out of the laminin polymer layer to bind nidogen-1 (Fig. 6). In true BMs, nidogen-1 bridges the laminin polymer and type IV collagen network. The collagen IV network showed an electron-dense layer in true BM (20). However, under the electron microscope, no electron-dense zone appeared in VMBM. In

true BMs, collagen IV α 1 and α 2 chains are most abundant forms of collagen IV and expressed in all BMs (19, 23). Immunohistochemical analysis showed that collagen IV protein was absent in the VMBM. Because of the absence of collagen IV, VMBM is only 40 to 50 nm thick, about half of that of true BMs.

Collagen IV is essential to the maintenance of BM integrity and functions. Collagen IV-deficient BMs are found in small amounts in newly formed ECs sprouts during the early steps of angiogenesis (49). Absence of collagen IV α 1 and α 2 chain genes causes structural deficiencies in BMs and failure of the integrity of Reichert’s membrane, resulting in death of the mouse embryo at the stages E10.5 to E11.5 (47). Mutants of collagen IV in the BMs cause the Goltz syndrome (3, 37). However, absence of collagen IV network does not affect BMs self-assembly (2) and, in true BMs, collagen IV networks have not been implicated in association with cellular receptors (50). Thus, the absence of collagen IV beneath the attached LECs may not affect the VMBM function to provide attaching sites for LECs. Nidogen-1 plays a role in cell attachment in true BMs (5, 34, 36, 53). In VMBM, nidogen-1 protein recruited by VP23R can provide the binding site for LECs. As other components in VMBM are identified in further studies, more attaching sites will also be discovered.

Based on the overlapping intercellular junctions (39, 43, 63), we identified the attached ECs as LECs. This result was confirmed by immunohistochemistry using specific antibody against Prox-1 (13, 44). The formation of VP23R-mimicked BMs and the attachment of LECs on the infected cells are unique phenomena that have never been found in viruses. Attached LECs enclose the infected cells like a bag. The functions of these infection signs need further studies. Under an electron microscope, an infected cell was observed to release endocytes and mature virions (Fig. 5G and H). One of the LECs uncovered the enclosed bag and allowed virions and endocytes to be released. The immunofluorescence assay at 6 dpi also demonstrated that the plasma membrane of the infected cells was still intact, even after all of the virions were released. The signals of VP23R also remained strong. Based on these results, we speculate that the attachment of LECs can segregate the infected cells from the host immune system. By encoding the laminin-like membrane protein VP23R, ISKNV generates a BM-like structure on the infected cells to house LECs, building a “camouflaged bunker” against the attack of host immune cells. This phenomenon is a unique strategy of virus to effectively shield from immune attacks. Further studies should be performed to confirm this hypothesis.

The process of LECs attaching to the infected cells may be similar to that of lymphangiogenesis, especially in pathological conditions, such as tumor metastasis, inflammation, and transplant rejection that involve migration and proliferation of ECs from preexisting vessels and recruitment and differentiation of bone marrow endothelial progenitor cells (33, 40, 56, 69). Although the precise molecular mechanisms that regulate lymphangiogenesis remain largely unknown, it is clear that some members of the vascular endothelial growth factor (VEGF)/platelet-derived growth factor (PDGF) family, such as VEGF-A, PDGF-BB, and particularly VEGF-C and VEGF-D, play important roles in this process (4, 22, 55, 56). Interestingly, it has been reported that the ISKNV genome contains an

ORF48R gene, which belongs to the VEGF/PDGF family and functions through the VEGF receptor, Flk-1 (60). Association of ORF48R with the origination of the attached LECs is worth of further studies.

Studies on VP23R functions elucidate the unique infection signs of megalocystiviruses. Functions of VP23R in attaching LECs to the surface of infected cells through VMBM can help us learn more about the pathogenetic mechanism of megalocystiviruses. This is essential for *Megalocystivirus* prevention and cure. Furthermore, in view of the unique profile of VMBM and unique behaviors of the attached LECs, many questions remain to be answered, such as are there any other components in VMBM and, if so, how do they function? Why did LECs, but not vascular ECs, appear on the surface of the infected cells? Where do the attached LECs come from? Further studies are necessary in order to answer these questions. The results are also important for studies of BM functions and lymphangiogenesis mechanisms.

ACKNOWLEDGMENTS

This research was supported by the National Natural Science Foundation of China under grants 30325035 and U0631008, the National Basic Research Program of China under grant 2006CB101802, the National High Technology Research and Development Program of China (863 Program) under grants 2006AA09Z445 and 2006AA100309, the Guangdong Province Natural Science Foundation under grant 20023002, the National Science Fund for Young Scholars under grant 30901114, and the Science and Technology Bureau of Guangdong Province.

REFERENCES

- Aumailley, M., C. Battaglia, U. Mayer, D. Reinhardt, R. Nischt, R. Timpl, and J. W. Fox. 1993. Nidogen mediates the formation of ternary complexes of basement membrane components. *Kidney Int.* **43**:7–12.
- Brauer P. R., and J. M. Keller. 1989. Ultrastructure of a model basement membrane lacking type IV collagen. *Anat. Rec.* **223**:376–383.
- Büchner, S. A., and P. Itin. 1992. Focal dermal hypoplasia syndrome in a male patient: report of a case and histologic and immunohistochemical studies. *Arch. Dermatol.* **128**:1078–1082.
- Cao, Y. 2005. Direct role of PDGF-BB in lymphangiogenesis and lymphatic metastasis. *Cell Cycle* **4**:228–230.
- Chakravarti, S., M. F. Tam, and A. E. Chung. 1990. The basement membrane glycoprotein ectactin promotes cell attachment and binds calcium ions. *J. Biol. Chem.* **265**:10597–10603.
- Chen, L. M., F. Wang, W. Song, and C. L. Hew. 2006. Temporal and differential gene expression of Singapore grouper iridovirus. *J. Gen. Virol.* **87**:2907–2915.
- Chinchar, V. G., S. Essbauer, J. G. He, A. Hyatt, T. Miyazaki, V. Seligy, and T. Williams. 2005. The double-stranded DNA viruses, family *Iridoviridae*, part II, p. 145–162. *In* C. M. Fauquet, M. A. Mayo, J. Maniloff, U. Desselberger, and L. A. Ball (ed.), *Virus Taxonomy: VIIIth Report of the International Committee on Taxonomy of Viruses*. Elsevier/Academic Press, London, United Kingdom.
- Darai, G., H. Deliu, J. Clark, H. Apfel, P. Schnitzler, and R. M. Flugel. 1985. Molecular cloning and physical mapping of the genome of fish lymphocystis disease virus. *Virology* **146**:292–301.
- Darai, G., K. Anders, H. G. Koch, H. Delius, H. Gelderblom, C. Samalecos, and R. M. Flugel. 1983. Analysis of the genome of fish lymphocystis disease virus isolated directly from epidermal tumours of pleuronectes. *Virology* **126**:466–479.
- Delius, H., G. Darai, and R. M. Flugel. 1984. DNA analysis of insect iridescent virus 6: evidence for circular permutation and terminal redundancy. *J. Virol.* **49**:609–614.
- Dong, C., S. Weng, X. Shi, X. Xu, N. Shi, and J. He. 2008. Development a mandarin fish *Siniperca chuatsi* fry cell line suitable for the study of infectious spleen and kidney necrosis virus (ISKNV). *Virus Res.* **135**:273–281.
- Fujiwara, S., H. Shinkai, K. Mann, and R. Timpl. 1993. Structure and localization of O- and N-linked oligosaccharide chains on basement membrane protein nidogen. *Matrix* **13**:215–222.
- Garrafa, E., L. Trainini, A. Benetti, E. Saba, L. Fezzardi, B. Lorusso, P. Borghetti, T. Bottio, E. Ceri, N. Portolani, S. Bonardelli, S. M. Giuliani, G. Annibale, A. Corradi, L. Imberti, and A. Caruso. 2005. Isolation, purification, and heterogeneity of human lymphatic endothelial cells from different tissues. *Lymphology* **38**:159–166.
- Go, J., M. Lancaster, K. Dece, O. Dhungyel, and R. Whittington. 2006. The molecular epidemiology of iridovirus in Murray cod (*Maccullochella peelii peellii*) and dwarf gourami (*Colisa lalia*) from distant biogeographical regions suggests a link between trade in ornamental fish and emerging iridoviral diseases. *Mol. Cell Probes* **20**:212–222.
- Han, R., M. Kanagawa, T. Yoshida-Moriguchi, E. P. Rader, R. A. Ng, D. E. Michele, D. E. Muirhead, S. Kunz, S. A. Moore, S. T. Iannaccone, K. Miyake, P. L. McNeil, U. Mayer, M. B. Oldstone, J. A. Faulkner, and K. P. Campbell. 2009. Basal lamina strengthens cell membrane integrity via the laminin G domain-binding motif of alpha-dystroglycan. *Proc. Natl. Acad. Sci. U. S. A.* **106**:12573–12579.
- He, J. G., K. Zeng, S. P. Weng, and S. M. Chan. 2000. Systemic disease caused by an iridovirus-like agent in cultured mandarin fish, *Siniperca chuatsi* (Basillewsky), in China. *J. Fish Dis.* **23**:219–222.
- He, J. G., K. Zeng, S. P. Weng, and S. M. Chan. 2002. Experimental transmission, pathogenicity and physical-chemical properties of infectious spleen and kidney necrosis virus (ISKNV). *Aquaculture* **204**:11–24.
- He, J. G., M. Deng, S. P. Weng, Z. Li, S. Y. Zhou, Q. X. Long, X. Z. Wang, and S. M. Chan. 2001. Complete genome analysis of the mandarin fish infectious spleen and kidney necrosis iridovirus. *Virology* **291**:126–139.
- Heidet, L., Y. Cai, L. Guicharnaud, C. Antignac, and M. C. Gubler. 2000. Glomerular expression of type IV collagen chains in normal and X-linked Alport syndrome kidneys. *Am. J. Pathol.* **156**:1901–1910.
- Henrikson, C. 1998. Urinary system, p. 203–223. *In* H. D. Dellman and J. Eurell (ed.), *Textbook of veterinary histology*, 5th ed. Lippincott/The Williams & Wilkins Co., Philadelphia, PA.
- Henry, M. D., J. S. Satz, C. Brakebusch, M. Costell, E. Gustafsson, R. Fässler, and K. P. Campbell. 2001. Distinct roles for dystroglycan, $\beta 1$ integrin, and perlecan in cell surface laminin organization. *J. Cell Sci.* **114**:1137–1144.
- Hirakawa, S., S. Kodama, R. Kunstfeld, K. Kajiya, L. F. Brown, and M. Detmar. 2005. VEGF-A induces tumor and sentinel lymph node lymphangiogenesis and promotes lymphatic metastasis. *J. Exp. Med.* **201**:1089–1099.
- Hudson, B. G., K. Tryggvason, M. Sundaramoorthy, and E. G. Neilson. 2003. Alport's syndrome, Goodpasture's syndrome, and type IV collagen. *N. Engl. J. Med.* **348**:2543–2556.
- Hudson, B. G., S. T. Reeders, and K. Tryggvason. 1993. Type IV collagen: structure, gene organization, and role in human diseases: molecular basis of Goodpasture and Alport syndromes and diffuse leiomyomatosis. *J. Biol. Chem.* **268**:26033–26036.
- Hultgårdh-Nilsson, A., and M. Durbeecj. 2007. Role of the extracellular matrix and its receptors in smooth muscle cell function: implications in vascular development and disease. *Curr. Opin. Lipidol.* **18**:540–545.
- Inouye, K., K. Yamano, Y. Maeno, K. Nakajima, M. Matsuoka, Y. Wada, and M. Sorimachi. 1992. Iridovirus infection of cultured red sea bream, *Pagrus major*. *Fish Pathol.* **27**:19–27.
- Iwata, M., Y. Sado, T. Sasaki, Y. Imamura, Y. Ninomiya, and T. Hayashi. 1996. The 160k alpha 1(IV) chain, a short form of a type IV collagen polypeptide, of bovine lens capsule retains the NC1 domain. *J. Biochem.* **120**:133–137.
- Jeong, J. B., H. Y. Kim, L. J. Jun, J. H. Lyu, N. G. Park, J. K. Kim, and H. D. Jeong. 2008. Outbreaks and risks of infectious spleen and kidney necrosis virus disease in freshwater ornamental fishes. *Dis. Aquat. Organ.* **78**:209–215.
- Jung, S. J., and M. J. Oh. 2000. Iridovirus-like infection associated with high mortalities of striped beakperch, *Oplegnathus fasciatus* (Temminck et Schlegel), in southern coastal areas of the Korean peninsula. *J. Fish Dis.* **23**:223–226.
- Kadoya, Y., K. Salmivirta, J. F. Talts, K. Kadoya, U. Mayer, R. Timpl, and P. Ekblom. 2003. Importance of nidogen binding to laminin gamma1 for branching epithelial morphogenesis of the submandibular gland. *Development* **124**:683–691.
- Kalluri, R. 2003. Basement membranes: structure, assembly and role in tumour angiogenesis. *Nat. Rev. Cancer* **3**:422–433.
- Kalluri, R., C. B. Wilson, M. Weber, S. Gunwar, A. M. Chonko, E. G. Neilson, and B. G. Hudson. 1995. Identification of the alpha 3 chain of type IV collagen as the common autoantigen in ant basement membrane disease and Goodpasture syndrome. *J. Am. Soc. Nephrol.* **6**:1178–1185.
- Kerjaschki, D., N. Huttary, I. Raab, H. Regele, K. Bojarski-Nagy, G. Bartel, S. M. Krober, H. Greinix, A. Rosenmaier, F. Karhofer, N. Wick, and P. R. Mazal. 2006. Lymphatic endothelial progenitor cells contribute to de novo lymphangiogenesis in human renal transplants. *Nat. Med.* **12**:230–234.
- Kim, S., and W. G. Wadsworth. 2000. Positioning of longitudinal nerves in *C. elegans* by nidogen. *Science* **288**:150–154.
- Kramer, J. M. 2005. Basement membranes. *WormBook* **2005**:1–15.
- Lee, H. K., I. A. Seo, H. K. Park, and H. T. Park. 2006. Identification of the basement membrane protein nidogen as a candidate ligand for tumor endothelial marker 7 in vitro and in vivo. *FEBS Lett.* **580**:2253–2257.
- Lee, I. J., M. S. Cha, S. C. Kim, and D. Bang. 1996. Electron microscopic

- observation of the basement membrane zone in focal dermal hypoplasia. *Pediatr. Dermatol.* **13**:5–9.
38. Li, S., P. Liguari, K. K. McKee, D. Harrison, R. Patel, S. Lee, and P. D. Yurchenco. 2005. Laminin-sulfatide binding initiates basement membrane assembly and enables receptor signaling in Schwann cells and fibroblasts. *J. Cell Biol.* **169**:179–189.
 39. Liu Z. Y., and J. R. Casley-Smith. 1989. The fine structure of the amphibian lymph sac. *Lymphology* **22**:31–35.
 40. Maruyama, K., M. Ii, C. Cursiefen, D. G. Jackson, H. Keino, M. Tomita, N. Van Rooijen, H. Takenaka, P. A. D'Amore, J. Stein-Streilein, D. W. Losordo, and J. W. Streilein. 2005. Inflammation-induced lymphangiogenesis in the cornea arises from CD11b-positive macrophages. *J. Clin. Invest.* **115**:2363–2372.
 41. Mayer, U., E. Kohfeldt, and R. Timpl. 1998. Structural and genetic analysis of laminin-nidogen interaction. *Ann. N. Y. Acad. Sci.* **857**:130–142.
 42. Mayer, U., R. Nischt, E. Pöschl, K. Mann, K. Fukuda, M. Gerl, Y. Yamada, and R. Timpl. 1993. A single EGF-like motif of laminin is responsible for high-affinity nidogen binding. *EMBO J.* **12**:1879–1885.
 43. Mendoza, E., and G. W. Schmid-Schönbein. 2003. A model for mechanics of primary lymphatic valves. *J. Biomech. Eng.* **125**:407–414.
 44. Parr, C., and W. G. Jiang. 2003. Quantitative analysis of lymphangiogenic markers in human colorectal cancer. *Int. J. Oncol.* **23**:533–539.
 45. Paulsson, M. 1992. Basement membrane proteins: structure, assembly, and cellular interaction. *Crit. Rev. Biochem. Mol. Biol.* **27**:93–127.
 46. Pöschl, E., J. W. Fox, D. Block, U. Mayer, and R. Timpl. 1994. Two non-contiguous regions contribute to nidogen binding to a single EGF-like motif of the laminin gamma 1 chain. *EMBO J.* **13**:3741–3747.
 47. Pöschl, E., U. Schlötzer-Schrehardt, B. Brachvogel, K. Saito, Y. Ninomiya, and U. Mayer. 2004. Collagen IV is essential for basement membrane stability but dispensable for initiation of its assembly during early development. *Development* **131**:1619–1628.
 48. Reinhardt, D., K. Mann, R. Nischt, J. W. Fox, M. L. Chu, T. Krieg, and R. Timpl. 1993. Mapping of nidogen binding sites for collagen type IV, heparan sulfate proteoglycan, and zinc. *J. Biol. Chem.* **268**:10881–10887.
 49. Sainson, R. C., J. Aoto, M. N. Nakatsu, M. Holderfield, E. Conn, E. Koller, and C. C. Hughes. 2005. Cell-autonomous notch signaling regulates endothelial cell branching and proliferation during vascular tubulogenesis. *FASEB J.* **19**:1027–1029.
 50. Sasaki, T., R. Fässler, and E. Hohenester. 2004. Laminin: the crux of basement membrane assembly. *JCB* **164**:959–963.
 51. Schéele, S., A. Nyström, M. Durbeecj, J. F. Talts, M. Ekblom, and P. Ekblom. 2007. Laminin isoforms in development and disease. *J. Mol. Med.* **85**:825–836.
 52. Schittny, J. C., and P. D. Yurchenco. 1989. Basement membranes: molecular organization and function in development and disease. *Curr. Opin. Cell Biol.* **1**:983–988.
 53. Senior, R. M., H. D. Gresham, G. L. Griffin, E. J. Brown, and A. E. Chung. 1992. Entactin stimulates neutrophil adhesion and chemotaxis through interactions between its Arg-Gly-Asp (RGD) domain and the leukocyte response integrin. *J. Clin. Invest.* **90**:2251–2257.
 54. Streuli, C. H., N. Bailey, and M. J. Bissell. 1991. Control of mammary epithelial differentiation: basement membrane induces tissue-specific gene expression in the absence of cell-cell interaction and morphological polarity. *J. Cell Biol.* **115**:1383–1395.
 55. Sugiura, T., Y. Inoue, R. Matsuki, K. Ishii, M. Takahashi, M. Abe, and K. Shirasuna. 2009. VEGF-C and VEGF-D expression is correlated with lymphatic vessel density and lymph node metastasis in oral squamous cell carcinoma: implications for use as a prognostic marker. *Int. J. Oncol.* **34**:673–680.
 56. Tammela, T., and K. Alitalo. 2010. Lymphangiogenesis: molecular mechanisms and future promise. *Cell* **140**:460–476.
 57. Tidona, C. A., and G. Darai. 1997. The complete DNA sequence of lymphocystis disease virus. *Virology* **230**:207–216.
 58. Utani, A., M. Nomizu, R. Timpl, P. P. Roller, and Y. Yamada. 1994. Laminin chain assembly: specific sequences at the C terminus of the long arm are required for the formation of specific double- and triple-stranded coiled-coil structures. *J. Biol. Chem.* **269**:19167–19175.
 59. Wang, Y. Q., L. Lu, S. P. Weng, J. N. Huang, S. M. Chan, and J. G. He. 2007. Molecular epidemiology and phylogenetic analysis of a marine fish infectious spleen and kidney necrosis virus-like (ISKNV-like) virus. *Arch. Virol.* **152**:763–773.
 60. Wang, Z. L., X. P. Xu, B. L. He, S. P. Weng, J. Xiao, L. Wang, T. Lin, X. Liu, Q. Wang, X. Q. Yu, and J. G. He. 2008. Infectious spleen and kidney necrosis virus ORF48R functions as a new viral vascular endothelial growth factor. *J. Virol.* **82**:4371–4383.
 61. Willem, M., N. Miosge, W. Halfter, N. Smyth, I. Jannetti, E. Burghart, R. Timpl, and U. Mayer. 2002. Specific ablation of the nidogen-binding site in the laminin gamma1 chain interferes with kidney and lung development. *Development* **129**:2711–2722.
 62. Williams, T. 1996. The iridoviruses. *Adv. Virus Res.* **46**:345–412.
 63. Witte, M. H., and C. L. Witte. 1987. Lymphatics and blood vessels, lymphangiogenesis and hemangiogenesis: from cell biology to clinical medicine. *Lymphology* **20**:257–266.
 64. Xu, X., L. Zhang, S. Weng, Z. Huang, J. Lu, D. Lan, X. Zhong, X. Yu, A. Xu, and J. He. 2008. A zebrafish (*Danio rerio*) model of infectious spleen and kidney necrosis virus (ISKNV) infection. *Virology* **376**:1–12.
 65. Yoshida-Moriguchi, T., L. Yu, S. H. Stalnaker, S. Davis, S. Kunz, M. Madison, M. B. Oldstone, H. Schachter, L. Wells, and K. P. Campbell. 2010. O-Mannosyl phosphorylation of α -dystroglycan is required for laminin binding. *Science* **327**:88–92.
 66. Yu, H., and J. F. Talts. 2003. β 1 integrin and α -dystroglycan binding sites are localized to different laminin-G-domain-like (LG) modules within the laminin α 5 chain G domain. *Biochem. J.* **371**:289–299.
 67. Yurchenco, P. D., P. S. Amenta, and B. L. Patton. 2004. Basement membrane assembly, stability and activities observed through a developmental lens. *Matrix Biol.* **22**:521–538.
 68. Yurchenco, P. D., Y. S. Cheng, and H. Colognato. 1992. Laminin forms an independent network in basement membranes. *J. Cell Biol.* **117**:1119–1133.
 69. Zumsteg, A., V. Baeriswyl, N. Imaizumi, R. Schwendener, C. Ruegg, and G. Christofori. 2009. Myeloid cells contribute to tumor lymphangiogenesis. *PLoS One* **4**:e7067.